

Variability and smoothing effects of PV power production

A literature survey

J. Widén

This report is part of the Smooth PV project - KTH

The core part of this report is the literature overview that was performed to get an overview of the research field and the most recent findings. The results of the survey are presented below, divided on observations of variability and smoothing in monitored data for PV power production, observations of variability and smoothing in solar radiation data and theoretical and empirically based models. For a summary and brief overview of the most important findings in the studies described below, see Appendix A.

Observed variability and smoothing in monitored PV data

Three recent studies from the American company SunEdison show empirically how the variability of the power output from PV system ensembles depends on the sizes of individual systems and on the geographical dispersion of systems. In Golnas and Voss (2010) PV system fleets in three service territories in the United States were studied; two in California and one in New Jersey. In total 67 PV systems, continuously monitored with a 1-min resolution, were considered in the study, with seven days in May chosen for the analysis. The systems were grouped in ensembles with different total capacities and some different compositions of systems for each total capacity, and three different metrics were used to quantify the variability for these ensembles. The reported variability, evaluated over one single day, is therefore related to whether the ensembles consist of many small or a few large systems giving the same total capacity within roughly the same area. More systems imply a higher dispersion over the service territory (at maximum 48, 96 and 98 km, respectively, between systems in each area), but no explicit relation to the degree of dispersion was evaluated.

The obvious finding is that power production restricted to one or a few sites is more variable than production dispersed on a large number of smaller systems. Table 1 summarises some illustrative results from the study, in this case the difference in maximum (negative) step change between the least and most dispersed PV ensembles for each ensemble capacity. The differences are dependent not only on the number of systems aggregated, but also on the composition of the ensemble (whether a few systems are dominating in terms of capacity or if there is an even distribution), the exact area for dispersion, and the irradiation variability on the actual day. Nevertheless, the table shows what smoothing can be achievable through distribution of PV systems. Distributing capacity around 1 MW_p over smaller, widely spread systems could lower maximum daily step changes from around 40-50 % of capacity to around 5 % of capacity. Note, however, that since only one day was studied for each ensemble, the

observed maximum step change is probably lower than what would appear over a longer observation period.

Table 1. Maximum PV step changes during one observed day in Golnas and Voss (2010). Note that the degree of dispersion depends both on the number of systems *and* whether one or a few systems are dominating, which is why the least dispersed ensembles can contain quite a few systems.

| Ensemble size (kW _p) | Least dispersed ensemble | | Most dispersed ensemble | |
|-------------------------------------|----------------------------------|----------------------|----------------------------------|----------------------|
| | Maximum 1-min step change (%) | Number of systems | Maximum 1-min step change (%) | Number of systems |
| 440 | 37 | 1 | 6 | 11 |
| 1000 | 17 | 15 | 8 | 17 |
| 1200 | 50 | 1 | 17 | 8 |
| 1200 | 43 | 2 | 5 | 15 |
| 2300 | 36 | 2 | 18 | 11 |
| 2500 | 21 | 20 | 8 | 22 |

This is apparent in Golnas et al. (2011), where the output of distributed PV systems in one service area in New Jersey was analysed over the longer period of 11 months with the same approach; the systems, 31 in total, were grouped in differently composed ensembles spread over different distances, at maximum 155 km between systems. In the study an analysis was also made for different time resolutions. The main result is naturally that the variability metrics increase systematically with increasing aggregation of individual systems, while the dependence on the time resolution is less coherent. As an example of the former, the maximum 1-min step change for the largest and most widely spread ensemble (1000 kW_p) is around 20 % of rated capacity while for a single system (440 kW_p) it is around 70 %. These maximum step changes are higher than in the previous study. Since an observed maximum is dependent on the observation period, a more suitable metric is to use a percentile of the distribution of the step changes. Golnas et al. (2011) use the 95th and 99.7th percentiles. For the most dispersed ensemble in this study the 95th percentile is 5 % of rated capacity and the 99.7th percentile is 11 %. As can be seen from those figures, another result is that the distribution of the step change is rather long-tailed, meaning that there are large jumps between the upper percentiles.

In the third study, Golnas and Bryan (2011) investigated the output fluctuations from a centralized PV plant that was Europe's largest at the time of writing. This plant, located in Rovigo, Italy, has a capacity of 70 MW_p in total and consists of 60 individual arrays, covering a total area of 850 000 m². In addition to the previous two studies, the authors systematically

analysed the impact of dispersion on variability (over relatively short distances, at maximum 1200 m between systems), as compared to the impact from capacity increases within the same limited area. This was done by on the one hand grouping the arrays into differently sized ensembles within the same area, and on the other hand considering ensembles of the same size dispersed on circles with different radii. The result was, naturally, that increased ensemble size dispersed within the same area does not decrease variability, whereas wider dispersion of the same capacity does. Dispersion of capacity along circles with radii from 100 to 600 m made the maximum observed step change over 9 months decrease from almost 70 % to around 45 % of capacity at the 1-min resolution. Note the difference to the previous studies, where the wider dispersion (maximum distances between systems in the order of 100 times longer) gave considerably lower maximum step changes.

A limited study of observed impacts of clouds on variability is provided by Kankiewicz et al. (2010). The study concerns a large PV plant covering 728 000 m² (180 acres) of land with a rated capacity of 25 MW_p, located in Florida. The analysis is based on electricity production data monitored at the 17 subsystems of the plant. The results presented are restricted to one day in December, but the time resolution of 10 seconds is higher than in the studies above. The impact of dispersion over the area of the plant can be clearly seen. The maximum 10-second step change observed over this day with passing clouds is around 60 % of capacity for individual subsystems (sized 0.8-1.6 MW_p) and around 5 % for the whole 25 MW_p system. The same figures for the 1-min resolution are around 40 % and 20 %, respectively. If observed over a longer period of time, the figures would probably be more similar to those of the Rovigo plant.

Two studies by Marcos et al. (2011a,c) analyse the impacts on variability from increasing system size and from increasing geographical dispersion of up to eight Spanish PV systems in the capacity range of 48 kW_p to 9.5 MW_p, over distances of up to 60 km. The analysis is more detailed than most of the previous ones and covers time resolutions from 1 second up to 10 minutes. The studies show both the variability of differently sized individual systems and of different aggregates of systems on variability. As an example, in Marcos et al. (2011a) the maximum 1-s step change is around 55 % of capacity for the smallest system (48 kW_p) and merely around 5 % for the largest system (9.5 MW_p), from one-year observations. The corresponding figures for the 1-min resolution are around 100 % and 70 %. The authors also report the 90th percentile of the step changes, plotted in Figure 1 against the plant area. As can be seen, there is considerable smoothing on the shorter time scales. Combining six systems within distances of 60 km further reduces the total variability. In Marcos et al. (2011c) the

99th percentiles are reported for all possible combinations of up to six plants. These decrease from around 10 % of capacity for one system to around 2 % for six systems at the 1-s resolution. The corresponding drop for the 1-min resolution is from 85 % to 35 %.

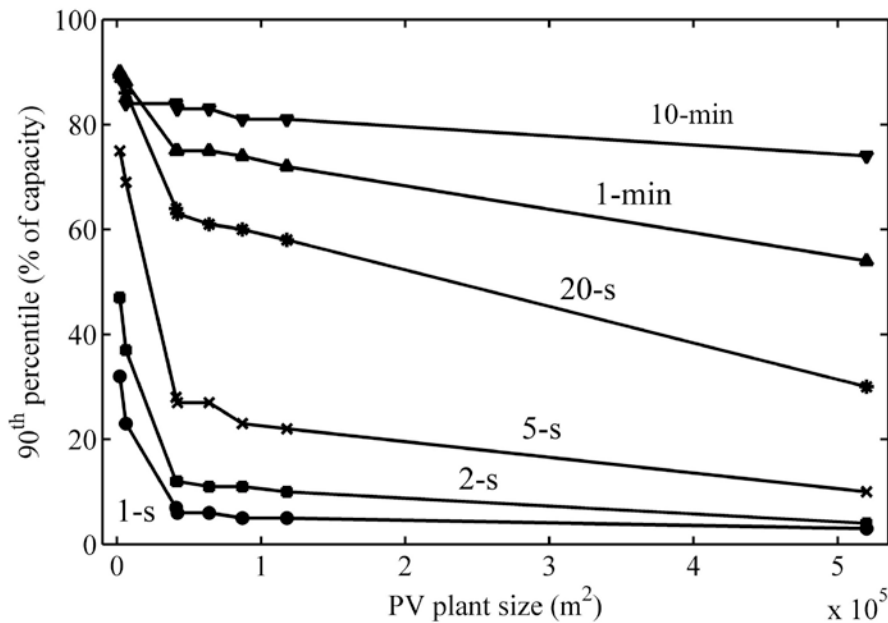


Figure 1. 90th percentile of step changes in the output from differently sized PV plants, based on values reported in Marcos et al. (2011a).

The latter study also uses these data to find empirical relations between the number of dispersed PV plants grouped, the 99th percentile of the step change, and the time resolution. The percentile decreases systematically with the dispersion and increases with the time resolution. For the extreme resolutions the decrease is from around 10 % of capacity to 2 % for the 1-s resolution, as mentioned, and from 90 % to 50 % for the 10-min resolution. In an attempt to generalize their findings the authors also fit their data to an empirical function relating the 99th percentile of the step change to the PV plant size and the number of dispersed systems (see below).

Two studies are also worth mentioning that consider the smoothing effect from dispersion over nation-wide distances. Murata et al. (2009) analysed electricity production data from 52 sites distributed over Japan. The main goal of the study was to relate the maximum step change to the standard deviation via empirically determined so-called fluctuation coefficients (see further discussion below). Wiemken et al. (2001) studied the electricity production from 100 PV systems spread over Germany, all monitored over one year with a 5-min resolution.

The main findings were that no step changes at this resolution were higher than 5 % of total capacity. Also, the aggregate power was never above 65 % of the total capacity.

Observed variability and smoothing in solar radiation data

Since PV variability depends directly on the variability in the irradiation on the solar cells, expected smoothing from geographical dispersion can also be determined from radiation data. An early study was made by Otani et al. (1997) using a Japanese radiation monitoring setup with 9 sites in a 4 x 4 km grid. The authors used a metric called the *fluctuation factor*, which is defined as the rms value of the fluctuations. With aggregation across the monitoring grid the authors could show that fluctuation factors based on 1-min data decreased by 40 % on average over one studied month and by 87 % at maximum. The same experimental setup was used by Kawasaki et al. (2006) to study the impact of different typical weather types on fluctuations and smoothing across the grid, showing distinctly different fluctuation patterns and degrees of smoothing on clear and rainy days and on days with moving clouds.

In a more recent study, Lave and Kleissl (2010) used measurements of global radiation on the horizontal plane at four sites in Colorado, located between 19 and 197 km apart, to study the smoothing effect. The maximum ramp rate, observed in 5-min data covering one whole year, was between 161 and 189 $\text{Wm}^{-2}\text{min}^{-1}$ for individual sites and 112 $\text{Wm}^{-2}\text{min}^{-1}$ for the four sites combined. As ramp rates in Wm^{-2} depend both on the sun's deterministic position in the sky and on cloud movements, it is customary to analyse the clearness index (actual radiation divided by the clear-sky radiation) rather than the absolute irradiance. Mills and Wiser (2010) used the clearness index determined from 1-min global horizontal radiation data covering one whole year to quantify the smoothing from dispersion of 23 PV sites over distances from 20 to 440 km. For example, the authors found that the 99.7th percentile dropped from 0.58 for one site to 0.19 for five sites, and to 0.09 for all 23 sites. Since the clearness index and the PV output relative to rated capacity are related, it is not surprising that these figures are comparable in size to the 99.7th percentile values for the PV output in Golnas et al. (2011) mentioned above.

Lave et al. (2011) used a one-month series of 1-s data for the clearness index at six sites, separated by less than 3 km, in San Diego, USA, to determine fluctuations on different time scales with a spectral analysis. Two metrics were used to characterize the variability; the *fluctuation power index* (fpi) and the *variability ratio* (VR). The fpi describes the power content in the fluctuations at each timescale. The VR is the fpi for one site divided by the fpi

for a set of aggregated sites. Thus, it shows the reduction in variability with aggregation. One of the results from the study is that the VR is around 6 (the number of sites) for short timescales and approaches 1 for longer timescales. This is analogous with the reduction in variability being equal to the number of sites for short timescales, for which the clearness indices are virtually uncorrelated, and with a slight or no reduction for longer timescales, for which the clearness indices are strongly correlated. The same thing can be seen in Figure 1 above where the plant size has less impact on the variability for longer times scales.

Theoretical and empirical models

Since widespread distributed PV has been extensively integrated in distribution systems just over the past one and a half decade, early studies used modeling techniques to determine the impact of moving clouds on aggregate PV generation. An early study was made by Jewell and Ramakumar (1987) who simulated clear-sky radiation and cloud movements to study the time to loss of all PV capacity in a service area due to movement of a squall line. Different service areas with uniformly distributed PV systems were considered. For example, the authors concluded that time for loss of all PV capacity during such an event was 1.8 min for a 10 km² area and 176 min for a 100 000 km² area.

Another early study on ramp rates in aggregate PV production was made by Kern et al. (1989). They used monitored PV production data from four individual systems combined with cloud models to find the aggregate power production from 28 PV systems and their total ramps during cloud passages. In total, 62 kW_p rated capacity was considered, spread over an area of 202 000 m² (50 acres). Over a whole cloud passage event, the average ramps were found to be 75 % of total capacity for a single system and 60 % for 28 systems. This corresponded to a ramp rate of 10 % per second for the single system and 3 % per second for 28 systems. Although hard to compare directly to the observed variability above, it is in the same order of magnitude observed e.g. for the systems in Figure 1.

More recent modeling efforts have tried to find generalized methods that can be used to determine the output variability in an arbitrarily large and arbitrarily distributed fleet of PV systems. Murata et al. (2009) suggested a partly empirical method to determine the maximum power fluctuation for an arbitrary aggregate of PV sites and implemented it, as mentioned, for Japanese nation-wide radiation data. In short, the model requires empirical data for the so-called *output fluctuation coefficient*, which is the ratio of the maximum step change to the standard deviation, and for the correlation coefficients between a representative number of

sites. By using the correlation data the standard deviation of an arbitrary set of sites can be determined, and the maximum step change can be found by multiplying this extrapolated standard deviation with the empirical output fluctuation coefficient. A percentile of the step changes for an arbitrary aggregate can be determined in the same way. The drawback of this method is of course the extensive data requirement.

A more elegant model based only on theoretical considerations was proposed by Hoff and Perez (2010) and is worth discussing in detail. The model is based on a variability metric called the *relative output variability*, which is the standard deviation of the Δt time step changes for the aggregate output from a fleet of N distributed PV systems ($\sigma_{\Delta t}^N$), divided by the standard deviation for the same fleet concentrated in one single location ($\sigma_{\Delta t}^1$). Another central concept is the dispersion factor, defined as

$$D = \frac{L}{V\Delta t}$$

where L is the extension of the PV fleet in the direction of cloud movement, V is the transit rate of clouds and Δt is the time resolution. The dispersion factor is thus the number of time intervals required for a cloud disturbance to pass over the whole PV fleet. The variability for this fleet of systems is dependent on the relative magnitudes of N and D . Four different cases can be defined:

1. The *spacious region*, $N \ll D$, where the output variability is independent between systems. The relative output variability in this region is inversely proportional to the square root of the number of systems:

$$\frac{\sigma_{\Delta t}^N}{\sigma_{\Delta t}^1} = \frac{1}{\sqrt{N}}$$

2. The *optimal point*, $N = D$, where a cloud shading one system will shade the next one in exactly one time step. At this point the relative output variability is

$$\frac{\sigma_{\Delta t}^N}{\sigma_{\Delta t}^1} = \frac{\sigma_{N\Delta t}^1}{\sigma_{\Delta t}^1} \frac{1}{N}$$

3. The *crowded region*, $N > D$, where a cloud affects more than one system of the fleet in one time interval. The relative output variability is then

$$\frac{\sigma_{\Delta t}^N}{\sigma_{\Delta t}^1} = \frac{\sigma_{D\Delta t}^1}{\sigma_{\Delta t}^1} \frac{1}{D}$$

4. Finally, the *limited region*, $N < D$, where a cloud disturbance does not reach the next PV system before the next time interval. For this region, no explicit expression for the relative output variability can be found, but a limiting value as D increases is the same as for the spacious region, i.e.

$$\frac{\sigma_{\Delta t}^N}{\sigma_{\Delta t}^1} = \frac{1}{\sqrt{N}}$$

A schematic outline of the relative output variability in these different regions is given in Figure 2.

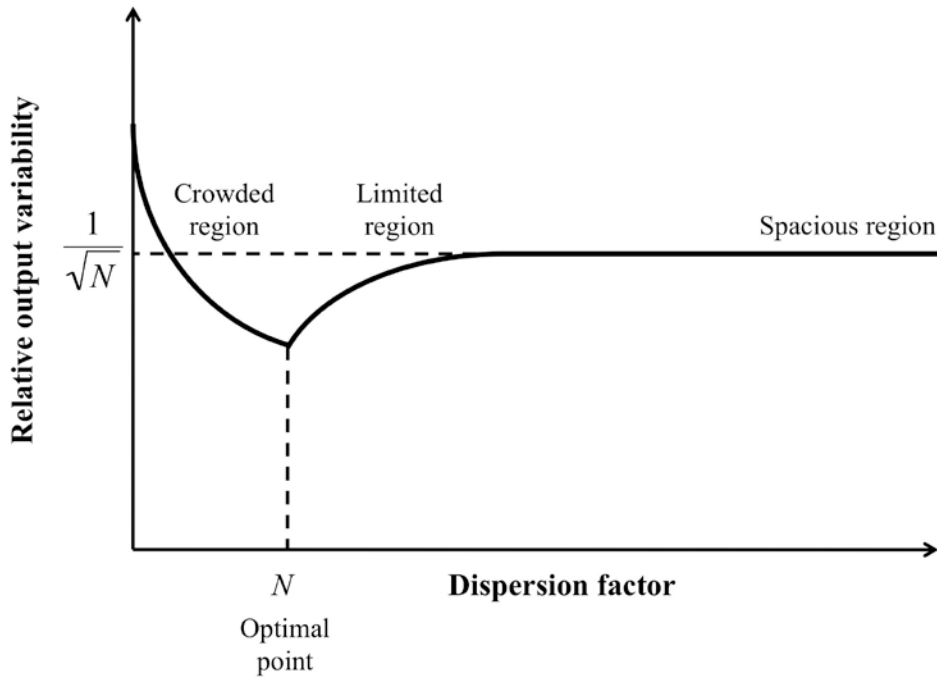


Figure 2. Schematic outline of the relative output variability as a function of the dispersion factor, with the different regions in the Hoff and Perez model indicated. Based on a similar outline in Hoff and Perez (2010).

Hoff and Perez use the theoretical model to determine the relative output variability in three scenarios where 100 MW_p PV capacity is distributed in different ways: one central power plant, 100 plants of 100 MW_p each and 20 000 plants of 5 kW_p each. The relative output

variability in these three scenarios was 18 %, 10 % and less than 1 %, respectively. An important observation is that the variability from the central power plant depends on the cloud transit rate and thus on the dispersion factor, while the variability from distributed systems depends on the number of systems.

These theoretical results are yet to be compared to data for real systems. Already, however, there have been attempts to test the validity of the model by some other authors. In an empirical model proposed by Marcos et al. (2011a,c) and fitted to the monitoring data already summarized above, the models for the crowded and spacious regions were reproduced. Already in Marcos et al. (2011a) it was noted that the curves shown in Figure 1 above could be fitted to exponential functions for the 90th percentile of the step change. Following the notation of Marcos et al., these functions are on the form:

$$90^{\text{th}}(\Delta P_{\Delta t, N}) = mS^{-c}$$

where S is the plant area, m is some proportionality constant and c is, for short time steps, equal to 0.5. This means that for high time resolutions the percentile decreases in proportion to $1/\sqrt{S}$. Noting that the square root of the plant area is the extension of the plant in one direction, this appears to correspond to the expression for the crowded region, where the output variability is inversely proportional to the dispersion factor D , which in turn is proportional to the plant extension L . For lower resolutions c approaches zero. This is also in line with the crowded region model, where the relative output variability approaches one for lower dispersion factors. This means that plant size does not influence the fluctuations on longer time scales, since clouds have time to pass over the whole plant within single time steps.

Marcos et al. (2011c) extend their empirical model to the 99th percentile of the step change for an arbitrary set of N sufficiently uncorrelated plants with plant areas S :

$$99^{\text{th}}(\Delta P_{\Delta t, N}) = 99^{\text{th}}(\Delta P_{600,1}) \left(1 - e^{-0.24\Delta t}\right)^{-c} N^{-a}$$

where $\Delta P_{600,1}$ is the hourly step change for one individual system. To obtain the parameters c and a the expression is fitted to data describing the smoothing with plant size and to data for the smoothing with site aggregation. As previously, for small Δt the c parameter turns out to

be close to 0.5 and for large Δt close to zero, analogous to the crowded region. For large Δt the a parameter is close to 0.5 and increases for shorter time scales. For the longer time scales this apparently corresponds to the Hoff and Perez model for the spacious region, because of the proportionality to $1/\sqrt{N}$. However, as the authors point out, the correlations between all considered sites was close to zero for all time scales, which suggests that the spacious region model should hold for all considered Δt . It is not entirely clear why the a parameter increases, but it might be an effect of the increasing total plant area, which provides further smoothing for high resolutions.

As Hoff and Perez, the authors use the model to extrapolate the 99th percentile of step changes for 100 MW_p PV capacity distributed in different ways. Some selected results are shown in Table 2. The value for the 1-min step changes can be compared to the empirical findings from the Rovigo system as reported by Golnas and Bryan (2011). The value estimated here for the centralized system is 70.9 % of capacity, whereas the maximum step change observed over 9 months for the Italian 70 MW_p plant apparently was around 45 %. One reason for the difference may be that the model, as admitted in the study, overestimates the percentile for larger areas and in particular for longer timescales (1-min and 10-min). Another reason could also be differences in local weather conditions and cloud movements.

Table 2. Calculated variability of 100 MW_p PV on different time scales (Marcos et al. 2011c).

| N | S (Ha) | 99 th percentile (% of total capacity) | | |
|--------|----------|---|-------|--------|
| | | 1-s | 1-min | 10-min |
| 1 | 651 | 0.9 | 70.9 | 86.1 |
| 10 | 65.1 | 0.5 | 18.6 | 31.3 |
| 100 | 6.51 | 0.2 | 4.9 | 11.3 |
| 1 000 | 0.651 | 0.1 | 1.3 | 4.1 |
| 10 000 | 0.0651 | 0.1 | 0.3 | 1.5 |

Appendix A

| Studies | Methodology (monitoring, simulation, etc.) | Data (time resolution, time period covered, number of systems, etc.) | Variability metrics (ramps, standard deviation, etc.) | PV system size / dispersion | Most important findings |
|----------------------------|--|---|--|--|--|
| Golnas and Voss (2010) | Statistical analysis of monitored electricity production | <ul style="list-style-type: none"> ▪ Electricity production from 67 systems in three service areas ▪ 1-min resolution ▪ 4 observed hours per day on 7 days in May 2010 | <ul style="list-style-type: none"> ▪ Standard deviation of step change ▪ Maximum power drop between time steps ▪ Fraction of step changes above 10 % of capacity | <ul style="list-style-type: none"> ▪ Differently sized ensembles of up to 22 systems ▪ Total capacities from 440 to 2500 kW_p ▪ Maximum distance between systems 98 km | <ul style="list-style-type: none"> ▪ Variability depends on ensemble size and composition ▪ Most power changes within 10 % of capacity ▪ For 2/3 of the ensembles more than 90 % of step changes below 10 % of capacity |
| Golnas et al. (2011) | Statistical analysis of monitored electricity production | <ul style="list-style-type: none"> ▪ Electricity production from 31 systems in one service area ▪ 1-, 10- and 60-min resolution ▪ 4 observed hours per day over 11 months, September 2010 – July 2011 | <ul style="list-style-type: none"> ▪ Maximum step change ▪ Distribution of step changes ▪ 95th and 99.7th percentiles of step changes | <ul style="list-style-type: none"> ▪ Differently sized ensembles of up to 23 systems ▪ Total capacities from 440 to 1000 kW_p ▪ Maximum distance between systems 155 km | <ul style="list-style-type: none"> ▪ Variability depends on ensemble size and composition ▪ For most distributed fleets 95 % of 1- and 10-min step changes below 10 % of capacity |
| Golnas and Bryan (2011) | Statistical analysis of monitored electricity production | <ul style="list-style-type: none"> ▪ Electricity production from 60 separate arrays of one large system ▪ 1-min to 60-min resolution ▪ 4 observed hours per day over 9 months, December 2010 – August 2011 | <ul style="list-style-type: none"> ▪ Standard deviation of step changes ▪ Maximum step change over monitoring period ▪ Step changes exceeding a certain magnitude | <ul style="list-style-type: none"> ▪ Differently sized ensembles of up to 60 arrays ▪ Total capacities from 6 MW_p to 70 MW_p ▪ Dispersion within a radius of up to 600 m | <ul style="list-style-type: none"> ▪ Variability depends on dispersion and not on total capacity ▪ Maximum step change 40-60 % of total capacity depending on time resolution ▪ Probability of step changes above 50 % of total capacity below 0.02 % for time steps between 1 min and 30 min |

| | | | | | |
|-----------------------------|--|--|---|--|---|
| Hoff and Perez (2010) | Modelling / simulation | Theoretically derived model relating PV output variability on different time scales to the so-called dispersion factor (number of time steps required for a cloud to pass the PV fleet) | Relative output variability: ratio of the standard deviation of step changes for a distributed PV fleet to the standard deviation for a single point location | Modelling of 100 MW PV capacity in three scenarios: <ul style="list-style-type: none"> • One central power plant • 100 plants, each 100 MW • 20 000 plants, each 5 kW | <ul style="list-style-type: none"> • Analytical formulas for the relative output variability for four different sizes of the dispersion factor in relation to the number of PV systems • In the three modelled scenarios, relative output variability is 18 %, 10 % and less than 1 %, respectively |
| Jewell and Ramakumar (1987) | Modelling / simulation | <ul style="list-style-type: none"> • Simulated clear-sky radiation and cloud movements • Time resolution from 6 seconds to 5 minutes | <ul style="list-style-type: none"> • Time to loss of all PV generation in a service area • Maximum loss of PV within a certain time frame | <ul style="list-style-type: none"> • Uniform distribution of PV systems within a service area (no exact capacity given) • Service areas from 10 km² to 100 000 km² | <ul style="list-style-type: none"> • Time for loss of all PV capacity due to a squall line range is 1.8 min for a 10 km² area and 176 min for a 100 000 km² area • During a 1 min interval 15.9 % of total PV capacity may be lost for a 10 km² area and 2.7 % for a 100 000 km² area |
| Kankiewicz et al. (2010) | Statistical analysis of monitored electricity production | <ul style="list-style-type: none"> • Electricity production from 17 subsystems within one large system • Time resolution from 10 seconds to 60 minutes • Analyzed data from one day (December 13, 2009) | Power step changes | <ul style="list-style-type: none"> • 17 containers (array groupings) of 0.8-1.6 MW_p within one system • Total capacity 25 MW_p • Covers 180 acres of land | <ul style="list-style-type: none"> • 10-sec maximum step changes around 60 % for individual containers, around 5 % for whole 25 MW_p site • 1-min step changes within 40 % of capacity for 1.6 MW_p, within 20 % for 25 MW_p • 10-min and 60-min step changes similar for 1.6 MW_p and 25 MW_p (within 40 %) |
| Kawasaki et al. (2006) | Statistical analysis of monitored radiation data | <ul style="list-style-type: none"> ▪ Global horizontal radiation from 9 sites ▪ 1-min resolution • Four days with different weather types (July and August 1997) | <ul style="list-style-type: none"> • Frequency distribution of fluctuations (Fourier transform) • Magnitude of fluctuations (Wavelet transform) | <ul style="list-style-type: none"> • 9 sites within a 4 × 4 km grid | <ul style="list-style-type: none"> • The largest fluctuations and the largest smoothing naturally appear on days with moving clouds • Clear and rainy days have the lowest fluctuations and the smallest smoothing |

| | | | | | |
|-------------------------|--|---|---|--|---|
| Kern et al. (1989) | Modelling / simulation | <ul style="list-style-type: none"> • Modelled electricity production of 28 aggregated systems, extrapolated with cloud models from 4 monitored systems • 1-s resolution • 10 minutes on one day (September 25, 1987) studied | <ul style="list-style-type: none"> • Average ramps during cloud passage events • Ramp rates per second during these events | <ul style="list-style-type: none"> • 28 systems, each with 2.2 kW_p rated power • Total rated capacity 61.6 kW_p • Spread over a 50 acre area | <ul style="list-style-type: none"> • Average ramps during cloud passage 75 % of total capacity for a single system, 60 % for 28 systems • Average ramp rates during cloud passages 10 % per second for a single system, 3 % per second for 28 systems |
| Lave and Kleissl (2010) | Statistical analysis of monitored radiation data | <ul style="list-style-type: none"> • Global horizontal radiation data of four sites • 5-min resolution • One whole year (2008) | <ul style="list-style-type: none"> • Statistical ramp rate metrics (maximum, mean, standard deviation) • Probability distribution of ramp rates | <ul style="list-style-type: none"> • Four sites • Distances between the sites range from 19 to 197 km | <ul style="list-style-type: none"> • Mean ramp rates are between 6.2 and 9.9 Wm⁻²min⁻¹ for single sites, 5.6 Wm⁻²min⁻¹ for the four sites combined • Maximum ramp rate is between 160.8 and 188.6 Wm⁻²min⁻¹ for single sites, 111.8 Wm⁻²min⁻¹ for the four sites combined |
| Lave et al. (2011) | Statistical analysis of monitored radiation data | <ul style="list-style-type: none"> • Clearness index at six sites • 1-s resolution • Almost one month (July 31 – August 25) | <ul style="list-style-type: none"> • Coherence spectra • Fluctuation power index (power content in fluctuations at each timescale) • Variability ratio for different time scales (reduction in variability with aggregation) | <ul style="list-style-type: none"> • Six sites • Distances between sites up to 3 km | <ul style="list-style-type: none"> • Variability ratio close to the number of sites for timescales shorter than about 4-min • Variability ratio nearly one for timescales longer than 1-h |
| Marcos et al. (2011a) | Statistical analysis of monitored electricity production | <ul style="list-style-type: none"> • Electricity production from 8 individual systems • 1-sec to 10-min resolution considered • One year, May 2008 – April 2009 | <ul style="list-style-type: none"> • Maximum power step changes • 90th percentile of step changes • Distributions of power step changes • Fitted empirical expression for 90th percentile step change as a function of plant size | <ul style="list-style-type: none"> • 8 separate systems with capacities ranging from 48 kW_p to 9.5 MW_p • Land area covered from 0.21 to 52 hectares • Distances between systems from 6 to 60 km | <ul style="list-style-type: none"> • Maximum 1-sec power step change is around 55 % for the smallest system and around 5 % for the largest system • Maximum 10-min step change is between 90 and 100 % for all systems • 90th percentile step change can be described by an exponential decay function with parameters dependent on the time resolution |

| | | | | | |
|-------------------------|---|---|--|--|--|
| Marcos et al. (2011c) | Statistical analysis of monitored electricity production | <ul style="list-style-type: none"> ▪ Electricity production from 7 individual systems ▪ 1-sec to 10-min resolution considered ▪ One year (2009) | <ul style="list-style-type: none"> ▪ Maximum power step changes ▪ 99th percentile of step changes ▪ Distributions of power step changes ▪ Fitted empirical expression for 99th percentile step changes as a function of plant size and number of sufficiently dispersed (uncorrelated) systems | <ul style="list-style-type: none"> ▪ Different combinations of 7 separate systems with capacities from 1 to 9.5 MW_p, 20 MW_p in total ▪ Land areas covered by system from 4.1 to 52 hectares ▪ Distances between 6 of the sites from 6 to 60 km, 7th site 320 km away | <ul style="list-style-type: none"> ▪ Maximum power fluctuations decrease from around 10 % for one system to around 2 % for 6 systems at 1-s time resolution, from 90 % to 50 % at 1-hour resolution ▪ Maximum power fluctuation for individual sites vary with system size from around 70 % for 1 MW_p to 30 % for 9.5 MW_p at 10-s resolution, from around 85 % to 70 % at 60-s ▪ 99th percentile step change can be empirically related to inverse powers of the system size and the number of dispersed systems |
| Mills and Wisser (2010) | Statistical analysis of monitored radiation data | <ul style="list-style-type: none"> ▪ Clear-sky index for 23 sites calculated from global horizontal radiation ▪ 1-min resolution ▪ One year (2004) | <ul style="list-style-type: none"> ▪ Cumulative distribution functions for step changes ▪ Statistical metrics of step changes (maximum, standard deviation, 99.7th percentile) | <ul style="list-style-type: none"> ▪ 23 sites ▪ Distance between sites from 20 to 440 km | <ul style="list-style-type: none"> ▪ Decrease in all statistical metrics with increasing aggregates, e.g. 99.7th percentile drops from 0.58 for one site to 0.19 for 5 sites, and to 0.09 for 23 sites at 1-min resolution ▪ The empirical distribution of step changes is more fat-tailed than a normal distribution but the similarity increases with aggregation |
| Murata et al. (2009) | Statistical analysis of monitored electricity production and radiation data | <ul style="list-style-type: none"> ▪ Electricity production and global horizontal radiation from 52 sites ▪ 1-min resolution ▪ 3 months (May, August, October) | <p>Two fluctuation coefficients based on step changes with different resolutions:</p> <ul style="list-style-type: none"> ▪ Ratio of maximum to standard deviation ▪ Ratio of 99.75th percentile to standard deviation | <ul style="list-style-type: none"> ▪ 52 sites spread over Japan ▪ Rated PV systems capacities from 0.12 to 5.6 kW, 3.2 kW on average | <ul style="list-style-type: none"> ▪ Extrapolated fluctuation coefficients for an infinite number of PV systems in a given region decrease with time resolution, e.g. the ratio of maximum to standard deviation is around 6-7 for 1-min and around 3 for 20-min ▪ The maximum step change from an arbitrary set of systems can be derived from the fluctuation coefficients and an analytical expression of the standard deviation |

| | | | | | |
|--------------------------|--|---|--|---|--|
| Otani et al. (1997) | Statistical analysis of monitored radiation data | <ul style="list-style-type: none"> ▪ Global horizontal radiation from 9 sites ▪ 1-min resolution ▪ One month (October 1996) / one day (May 16, 1996) | <ul style="list-style-type: none"> ▪ Fluctuation factor (rms value of the fluctuations) ▪ Power spectral density | <ul style="list-style-type: none"> ▪ 9 sites within a 4 × 4 km grid | <ul style="list-style-type: none"> ▪ Daily fluctuation factors decrease by 40 % on average over one month and by 87 % at maximum ▪ Power spectral density peaks and average values decrease with aggregation |
| Wiemken et al. (2001) | Statistical analysis of monitored electricity production | <ul style="list-style-type: none"> ▪ Electricity production from 100 systems ▪ 5-min resolution ▪ One year (1995) | <ul style="list-style-type: none"> ▪ Frequency distribution of ramps ▪ Output power distribution | <ul style="list-style-type: none"> ▪ 100 individual 1-5 kW_p systems ▪ 243 kW_p in total ▪ Spread out over Germany, 600 × 750 km² | <ul style="list-style-type: none"> ▪ No ramps above 5 % of total capacity ▪ Power levels below 65 % of total capacity |
